Patterning of frontal cortex subdivisions by Fgf17

Jeremy A. Cholfin*†‡§ and John L. R. Rubenstein‡§¶

*Medical Scientist Training Program, †Neuroscience Graduate Program, ‡Nina Ireland Laboratory of Developmental Neurobiology, and §Department of Psychiatry, University of California, San Francisco, CA 94143-2611

Communicated by Pasko Rakic, Yale University School of Medicine, New Haven, CT, March 14, 2007 (received for review February 7, 2007)

The frontal cortex (FC) is the seat of higher cognition. The genetic mechanisms that control formation of the functionally distinct subdivisions of the FC are unknown. Using a set of gene expression markers that distinguish subdivisions of the newborn mouse FC, we show that loss of *Fgf17* selectively reduces the size of the dorsal FC whereas ventral/orbital FC appears normal. These changes are complemented by a rostral shift of sensory cortical areas. Thus, *Fgf17* functions similar to *Fgf8* in patterning the overall neocortical map but has a more selective role in regulating the properties of the dorsal but not ventral FC.

arealization | regionalization | forebrain | protomap | neocortex

The frontal cortex (FC) consists of prefrontal, premotor, and motor areas that play a central role in cognition, movement, and behavior (1). The adult rodent prefrontal cortex (PFC) can be divided into medial and orbital regions that are thought to have homologues in primates (2). The medial PFC (mPFC) can be further subdivided into the dorsal mPFC, which includes frontal association, anterior cingulate, and dorsal prelimbic areas; and the ventral mPFC, which consists of ventral prelimbic, infralimbic, and medial orbital areas (3). The developmental mechanisms that generate FC subdivisions are unknown, in part, because of the lack of markers that distinguish these regions. In addition, most known mouse mutants that affect cortical patterning die at birth, precluding later analysis, when individual areas are distinguishable by classical histological methods.

Current evidence shows that neocortical areas are presaged by regionalized expression of transcription factors and other regulatory genes in the cortical neuroepithelium and cortical plate, supporting the protomap model (4–7). Members of the fibroblast growth factor (*Fgf*) family of genes have been implicated in controlling neocortical regionalization. *Fgf8* and *Fgf17* encode secreted signaling proteins and are expressed in a partially overlapping pattern in the rostral forebrain patterning center immediately adjacent to the developing FC [Fig. 1*A* and supporting information (SI) Fig. 7] (8–11). *Fgf8* patterns the neocortex in part by regulating the expression of transcription factor gradients in the cortical neuroepithelium (7, 12–16). Although ectopic expression of *Fgf17* has been reported to have effects similar to that of *Fgf8* in mediating overall patterning of the neocortical map (13), the role of endogenous *Fgf17* in forebrain development is unknown.

In this study we devised a panel of gene expression markers to examine the role of *Fgf17* in the regionalization of the rodent FC using *Fgf17*-null mice ($Fgf17^{-/-}$) (17). We report that the dorsal FC of $Fgf17^{-/-}$ mice was reduced in size, whereas ventral and orbital FC regions appeared normal. The reduction in the dorsal FC area was complemented by a rostromedial shift of caudal cortical areas. These changes in regionalization persisted into adulthood and were accompanied by a reduction in FC projections to subcortical targets. Thus, in addition to an overall effect on neocortical patterning, *Fgf17* has an unexpectedly selective role in regulating dorsal FC development.

Results

We examined *Fgf8* expression in the rostral patterning center of $Fgf17^{-/-}$ mutants given *Fgf8*'s important function in telencephalic patterning (12, 14–16). At embryonic day 10.5, telencephalic expression of *Fgf8* appeared the same in wild-type and $Fgf17^{-/-}$ littermate embryos (Fig. 1 *C* and *C′*), suggesting that *Fgf17* does not affect cortical development by regulating *Fgf8* expression.

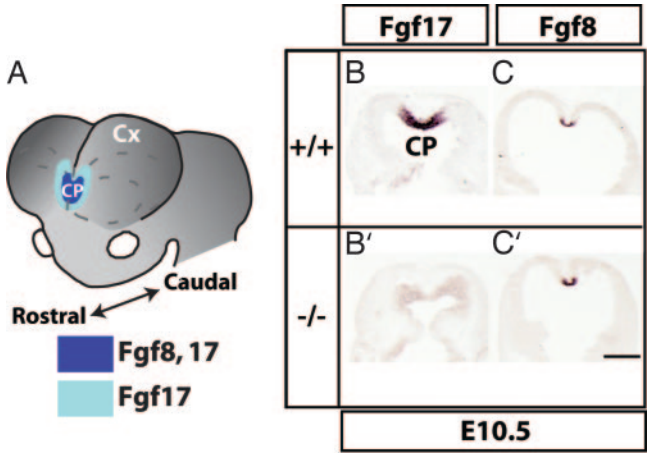

Fig. 1. *Fgf8* and *Fgf17* expression overlap in the forebrain rostral patterning center, and *Fgf8* expression is maintained in the $Fgf17^{-/-}$ mutant. (*A*) *Fgf17* and *Fgf8* RNA expression in the rostral forebrain patterning center. CP, commissural plate; Cx, cortex. (*B*, *B′*, *C*, and *C′*) *Fgf17* and *Fgf8 in situ* hybridization (ISH) on horizontal sections from embryonic day 10.5 $Fgf17^{+/+}$ (*B* and *C*) and $Fgf17^{-/-}$ (*B′* and *C′*) forebrain. Rostral is at the top. (Scale bar: 0.5 mm.)

The $Fgf17^{-/-}$ forebrain lacked overt morphological defects (SI Fig. 8 *A*, *A′*, *B*, and *B′*). Although we found no significant difference in cortical surface area in postnatal day 0 (P0) brains (SI Fig. 8*C*), adult cortical surface area was slightly (≈7%) reduced (SI Fig. 8*D*). In addition, the olfactory bulbs and basal ganglia, which are severely reduced in $Fgf8^{neo/neo}$ and $Fgf8^{neo/null}$ hypomorphic mutants, respectively (14, 16), are roughly normal in size and exhibited no differences in histology or gene expression in $Fgf17^{-/-}$ mutants (SI Fig. 9). This suggests that, compared with *Fgf8*, *Fgf17* has only a minor role in regulating the overall growth of the telencephalon.

To assess whether the $Fgf17^{-/-}$ mutation altered rostral parts of the telencephalon, we focused on the FC. To this end, we introduced BAC-EphA2 and BAC-Drd4 alleles, which express GFP in specific FC domains (18). $Fgf17^{-/-}$ mice at P0, P7, and P8 had a smaller domain of FC GFP fluorescence (Fig. 2 *A*, *A′*,

Author contributions: J.A.C. and J.L.R.R. designed research; J.A.C. performed research; J.L.R.R. contributed new reagents/analytic tools; J.A.C. and J.L.R.R. analyzed data; and J.A.C. and J.L.R.R. wrote the paper.

The authors declare no conflict of interest.

Abbreviations: FC, frontal cortex; PFC, prefrontal cortex; mPFC, medial PFC; P*n*, postnatal day *n*; DiI, 1,1′-dioctadecyl 3,3,3′,3′-tetramethylindocarbocyanine perchlorate; ISH, *in situ* hybridization.

¶To whom correspondence should be addressed at: University of California, Rock Hall Room #282, 1550 Fourth Street, San Francisco, CA 94143-2611. E-mail: john.rubenstein@ucsf.edu.

This article contains supporting information online at www.pnas.org/cgi/content/full/0702225104/DC1.

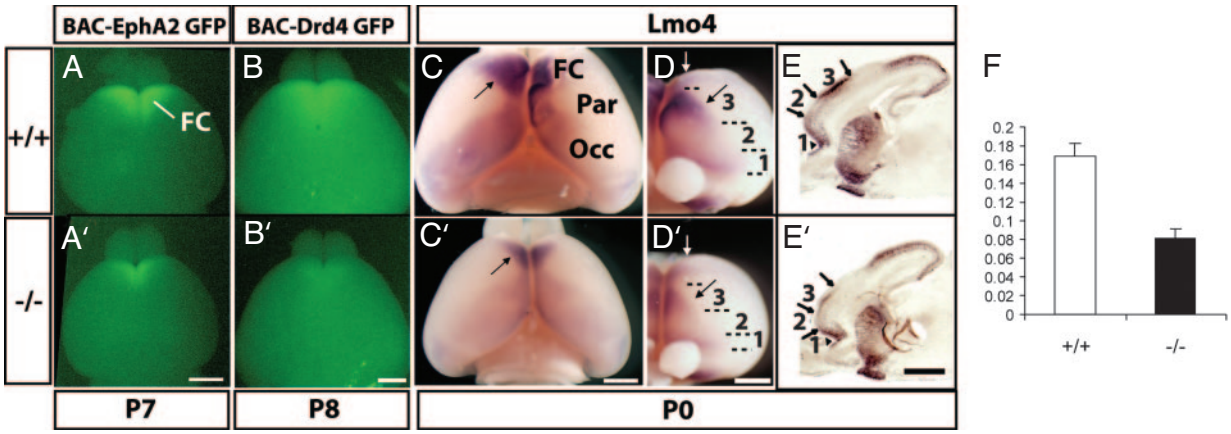

Fig. 2. Reduced FC size in *Fgf17*$^{-/-}$ mice. Arrows signify shifted boundaries, and arrowheads signify maintained boundaries. (*A* and *A′*) Dorsal views of P7 *Fgf17*$^{+/+}$ and *Fgf17*$^{-/-}$ brains positive for the BAC-EphA2 GFP transgene. The GFP+ domain that marks the FC was reduced in *Fgf17*$^{-/-}$ mutants. (*B* and *B′*) Dorsal views of P8 *Fgf17*$^{+/+}$ and *Fgf17*$^{-/-}$ brains positive for the BAC-Drd4 GFP transgene. (*C* and *C′*) Dorsal views of *Lmo4* whole-mount ISH on P0 *Fgf17*$^{+/+}$ and *Fgf17*$^{-/-}$ brains. Par, parietal cortex; Occ, occipital cortex. (*D* and *D′*) Frontal views of the same brains in *C* and *C′* reveal gene expression boundaries that distinguish three early FC subdivisions that we have labeled 1–3. (*E* and *E′*) Sagittal sections processed for *Lmo4* ISH on P0 *Fgf17*$^{+/+}$ and *Fgf17*$^{-/-}$ brains reveal sharp gene expression boundaries within the FC. White arrows in *D* and *D′* indicate the approximate plane of section in *E* and *E′*. (*F*) Ratio of *Lmo4*+ dorsal FC area to total cortex area in *Fgf17*$^{+/+}$ ($n = 4$) and *Fgf17*$^{-/-}$ ($n = 4$) P0 hemispheres (Student's *t* test; $t = 5.21$ and $P < 0.01$). (Scale bars: 1 mm.)

B, and *B′* and data not shown), suggesting a decrease in FC size. We similarly observed reduced dorsal FC *Lmo4* RNA expression in *Fgf17*$^{-/-}$ whole-mount brains at P0 (Fig. 2 *C*, *C′*, *D*, and *D′*), providing evidence that the small FC is not due to the BAC transgene. *Lmo4*+ dorsal FC area was reduced by 52% after correcting for overall cortex size (Fig. 2*F*). Interestingly, *Lmo4* expression in the medial and orbital FC was not overtly affected (Fig. 2 *D* and *D′*), suggesting that *Fgf17* has a selective role in patterning FC subdivisions.

To distinguish between a reduction in expression levels and a shift in area properties, we examined *Lmo4* expression in sagittal sections. We observed no change in the level of *Lmo4* RNA or in the layer-specific pattern, but rather a rostral shift of the sharp borders that approximate neocortical areal subdivisions (Fig. 2 *E* and *E′*). In the sagittal view the dorsal FC domain was rostrally shifted (3 in Fig. 2 *E* and *E′*), whereas the ventral domain was less affected (1 in Fig. 2 *E* and *E′*). Other brain structures such as the striatum, olfactory tubercle, and hippocampus displayed normal *Lmo4* expression.

We explored the possibility that *Fgf17* has a selective role in dorsal FC patterning using a panel of gene expression markers on a series of coronal sections that span the FC at P0 (Fig. 3 and SI Figs. 10 and 11). Based on the expression domains and complementary borders of BAC-Drd4 GFP, *Lmo4*, *Cad8*, *Nt3*, *Steel*, *Ngn2*, *Rzr-β*, *Cad6*, *Lmo3*, *EphrinA5*, and *Id2*, we distinguished subdivisions in the rostral cortex that correlate with presumptive anatomical cortical areas (Fig. 3*A*, SI Fig. 10, Table 1, and SI Table 2). In the dorsal cortex we defined three FC

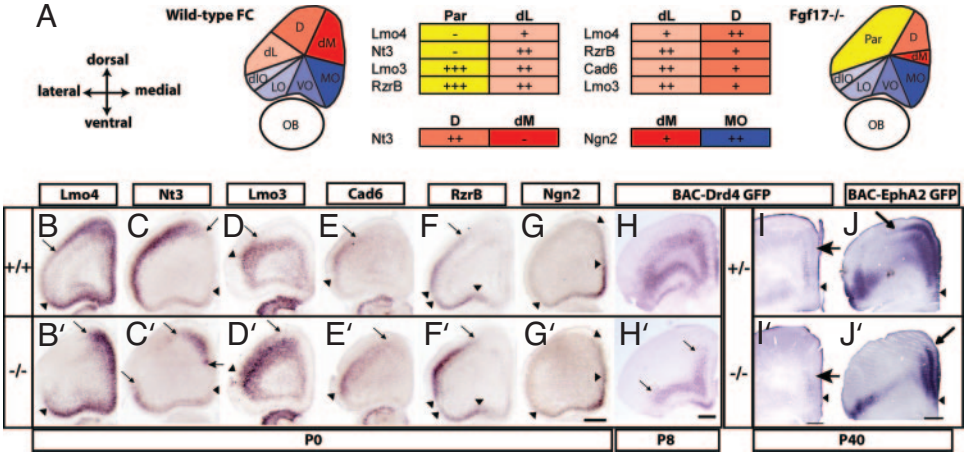

Fig. 3. Selective changes in dorsal FC molecular properties revealed by a panel of gene expression markers. Arrows signify shifted boundaries, and arrowheads signify maintained boundaries. (*A*) Schema of wild-type and *Fgf17*$^{-/-}$ mutant FC subdivisions based on a panel of gene expression markers at P0. Dorsal and ventral FC subdivisions are shaded in red and blue, respectively. The parietal cortex is shaded in yellow. The table focuses on key wild-type subdivision distinctions with levels of expression for each gene: +++, strong expression; ++, moderate expression; +, weak expression; −, no detectable expression. See Table 1 for corresponding anatomical areas and SI Tables 2 and 3 for a more detailed analysis. (*B–G* and *B′–G′*) ISH for *Lmo4*, *Nt3*, *Lmo3*, *Cad6*, *Rzr-β*, and *Ngn2* on *Fgf17*$^{+/+}$ and *Fgf17*$^{-/-}$ littermate P0 coronal sections. Note the shift in dorsal expression borders (arrows) but maintenance of ventral borders (arrowheads). (*H*, *H′*, *I*, and *I′*) Anti-GFP immunohistochemistry on coronal sections from P8 (*H* and *H′*) and P40 (*I* and *I′*) mice containing the BAC-Drd4 GFP transgene. Note that the expression is much broader in the FC at P8 but is restricted in the mPFC at P40. (*J* and *J′*) Anti-GFP immunohistochemistry on coronal sections from P40 mice containing the BAC-EphA2 GFP transgene. D, dorsal FC; dlO, dorsolateral orbital cortex; dM, dorsomedial FC; LO, lateral orbital cortex; MO, medial orbital cortex; Par, parietal cortex; VO, ventral orbital cortex. (Scale bars: 0.5 mm.)

Table 1. Frontal cortex subdivision definitions

Gene-defined region	Anatomical areas	
	Zilles and Wree (40)	Krettek and Price (41)
Dorsolateral	Fr1, Fr3	PrCl
Dorsal	Fr1, Fr2	PrCl, PrCm
Dorsomedial	Cg1, Cg2, Cg3	ACd, ACv, PL
Infralimbic	IL	IL
Medial orbital	MO	MO
Ventral orbital	VO	VO
Lateral orbital	LO	LO
Dorsolateral orbital	DLO	DLO
Agranular insular	AID/AIV	AId/AIv
Parietal	Par1	S1

subdivisions, dorsomedial, dorsal, and dorsolateral, and a single parietal cortex subdivision, whereas the ventral FC consisted of orbital subdivisions (medial orbital cortex, ventral orbital cortex, lateral orbital cortex, and dorsolateral orbital cortex), and more caudally the agranular insular and infralimbic areas (Fig. 3*A*, SI Fig. 10, Table 1, and SI Table 2).

We used this gene expression panel to determine how individual regional FC subdivisions were altered in P0 *Fgf17*$^{-/-}$ mutants. In this analysis we compared matched coronal sections (Fig. 3) and a whole series of coronal sections (SI Figs. 10 and 11). We focused on some key subdivision distinctions that showed the most obvious changes in gene expression (Fig. 3*A* and SI Table 3). *Fgf17*$^{-/-}$ mice had medially shifted dorsal FC expression borders of *Lmo4*, *Nt3*, BAC-Drd4 GFP, and *Cad8* (Fig. 3 *B*, *B′*, *C*, and *C′* and SI Figs. 10 and 11), whereas parietal cortex markers *Lmo3*, *Cad6*, *Rzr-β*, and *EphrinA5* showed a complementary expansion from more caudal cortex into this region (Fig. 3 *D*, *D′*, *E*, *E′*, *F*, and *F′* and SI Figs. 10 and 11). By contrast, the ventral FC showed no changes in gene expression (Fig. 3 and SI Figs. 10 and 11). Together, the pattern of changes suggests that subdivisions of the dorsal FC (dorsal, dorsolateral, and dorsomedial regions) are reduced, the parietal cortex expands into the FC, and ventral FC subdivisions are not affected (Fig. 3*A* and SI Fig. 11). This provides strong evidence that *Fgf17* has a selective role in regulating the regional properties of the dorsal but not ventral FC.

To explore further whether there is a rostral shift of caudal cortical regions, we examined gene expression in P0 sagittal sections. This revealed a rostral shift of parietal and occipital domains delimited by *Lmo4* and *Lmo3* expression (Fig. 4 *A*, *A′*, *B*, and *B′* and SI Fig. 12). These observations were confirmed at P7 based on a rostral shift of the somatosensory and visual cortex in flat-mount preparations stained for cytochrome oxidase and 5-hydroxytryptamine (5-HT, serotonin) (Fig. 4 *C*, *C′*, *D*, and *D′*) (19). Therefore, in addition to regulating the size of dorsal FC areas, *Fgf17* controls the position of sensory neocortical areas along the rostral–caudal axis.

Next we assessed whether these early postnatal alterations in cortical areas were observed in the mature brain by examining expression of BAC-Drd4 GFP and BAC-EphA2 GFP in P40 and 6-month-old mice. At P40, BAC-Drd4 GFP labeled a discrete domain of cells in the medial FC that correlates with the prelimbic area (Figs. 3*I* and 5*B*) (20). Although the position of the ventral border and layer-specificity of GFP+ cells was maintained, the extent of this domain was reduced in the *Fgf17*$^{-/-}$ brain (Figs. 3*I′* and 5*B′*), suggesting that the prelimbic cortical area (ventral part of dorsomedial region) is reduced in size. At P40 and in 6-month-old mice, BAC-EphA2 GFP labels the PFC (including frontal association, anterior cingulate, prelimbic, and infralimbic areas) (Figs. 3*J* and 5 *A* and *C* and SI Figs. 13 and 14). In the *Fgf17*$^{-/-}$ mutant, the dorsal expression border was shifted medially, whereas the ventral border was maintained (Figs. 3*J′* and 5*A′* and *C′* and SI Figs. 13 and 14), confirming that the PFC is smaller.

The dorsal FC sends projections through the dorsal striatum, which can be visualized in mice expressing BAC-EphA2 GFP (3, 18). In *Fgf17*$^{+/-}$ BAC-EphA2 GFP+ mice, GFP+ fiber staining is apparent throughout most of the dorsal striatum (Fig. 5*A* and SI Fig. 13). However, in *Fgf17*$^{-/-}$ mice, GFP+ fiber labeling in the dorsolateral striatum appeared reduced, consistent with the smaller domain of BAC-EphA2 GFP+ cells in the dorsal FC (Fig. 5*A′* and SI Fig. 13).

BAC-EphA2 GFP is expressed at higher levels in the somatosensory cortex and at lower levels in the motor cortex at P180 (Fig. 5*C*). The sensory–motor boundary was shifted to a more rostral position in the *Fgf17*$^{-/-}$ cortex (dashed arrows in Fig. 5 *C* and *C′*). Consistent with this gene expression shift, cytochrome oxidase staining of adjacent sections revealed that the somatosensory barrels were shifted rostrally in the *Fgf17*$^{-/-}$ mutant (SI Fig. 14). Together, these findings suggest that the early pattern of changes in regional molecular properties (Figs. 2–4) results in a permanent change in the distribution of adult cortical areas.

A subset of FC projections extends to the substantia nigra pars compacta and adjacent ventral tegmental area (3). These projections can be visualized in mice expressing the BAC-Drd4 GFP transgene (Fig. 6*A* and SI Fig. 15) (18). Staining of these projections was reduced in the *Fgf17*$^{-/-}$ mutant (Fig. 6*A′*), consistent with the reduction of BAC-Drd4 GFP+ cells in the FC (Fig. 3*H′* and SI Fig. 11). This suggests that the *Fgf17*$^{-/-}$

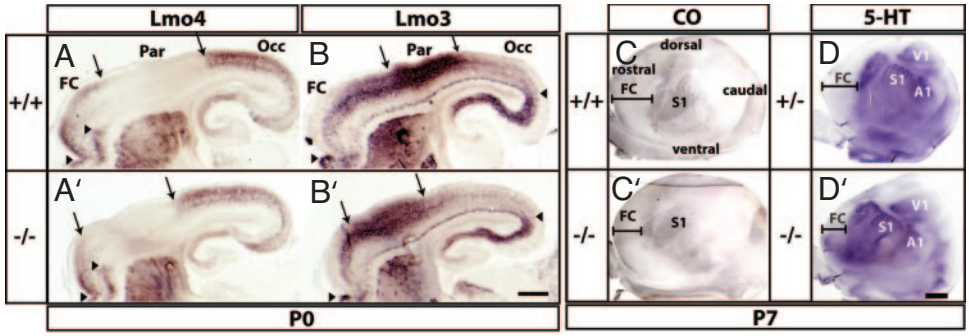

Fig. 4. Rostral shift of the neocortical map in *Fgf17*$^{-/-}$ mutants. Rostral is to the left. Arrows signify shifted boundaries, and arrowheads signify maintained boundaries. (*A*, *A′*, *B*, and *B′*) *Lmo4* and *Lmo3* ISH on sagittal sections from *Fgf17*$^{+/+}$ and *Fgf17*$^{-/-}$ P0 brains mark complementary cortical domains: frontal/occipital (FC/Occ) and parietal (Par) cortex, respectively. (Scale bar: 0.5 mm.) (*C*, *C′*, *D*, and *D′*) Cytochrome oxidase (CO) and anti-serotonin (5-HT) immunohistochemistry on tangential sections of flattened P7 cortices reveal a rostrodorsal shift of primary sensory areas. S1, somatosensory; V1, visual; A1, auditory. (Scale bar: 1 mm.)

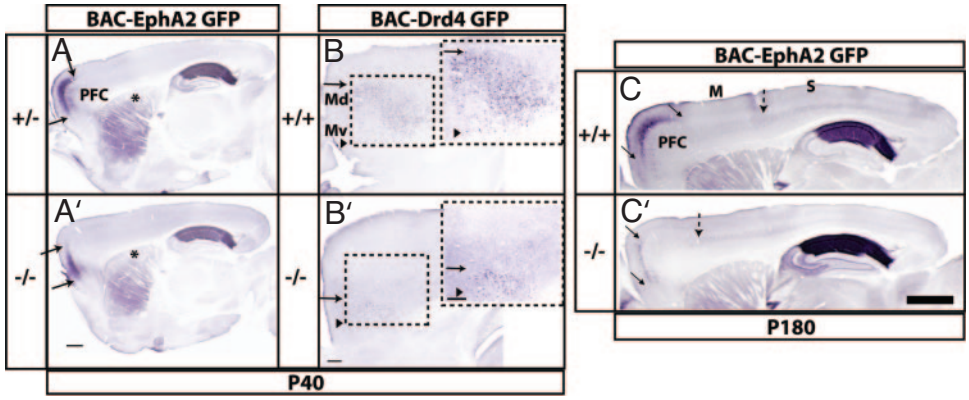

Fig. 5. Persistence of changes in FC molecular regionalization in mature *Fgf17*$^{-/-}$ mice. Arrows signify shifted boundaries, and arrowheads signify maintained boundaries. (*A*, *A′*, *B*, and *B′*) Sagittal sections of brains from P40 mice carrying either the BAC-EphA2 GFP or BAC-Drd4 GFP transgene processed for anti-GFP immunohistochemistry. Fiber staining in the dorsal striatum in BAC-EphA2 GFP+ mice corresponds to projections from the FC (asterisks in *A* and *A′*). Boxed areas, consisting of dorsomedial (Md) and ventromedial (Mv) subdivisions of the PFC, are shown in a magnified view (*Right Insets* in *B* and *B′*). (Scale bars: 0.5 mm.) (*C* and *C′*) Sagittal sections of cortex from adult (P180) BAC-EphA2+, *Fgf17*$^{+/+}$, and *Fgf17*$^{-/-}$ mice processed for anti-GFP immunohistochemistry. The broken arrow approximates the sensory (S)–motor (M) boundary. (Scale bar: 1 mm.)

mutation has a quantitative effect on dorsal FC cell number but does not have an overt qualitative effect on the pathfinding properties of the remaining BAC-Drd4 GFP+ axons. Furthermore, despite the reduction in BAC-Drd4 GFP+ FC axons, staining for tyrosine hydroxylase, a marker of midbrain dopamine neurons, did not show a discernable change (Fig. 6 *B* and *B′*), suggesting that the *Fgf17*$^{-/-}$ mutation does not overtly affect midbrain dopamine cell number.

Finally, we examined immature FC connectivity in P0 and P3 *Fgf17*$^{+/+}$ and *Fgf17*$^{-/-}$ mutant brains using the lipophilic dye (1,1′-dioctadecyl 3,3,3′,3′-tetramethylindocarbocyanine perchlorate (DiI) (Fig. 6 and SI Fig. 16). Placement of DiI crystals in the mPFC (Fig. 6*C* and SI Fig. 16) (dorsomedial and ventromedial regions) labeled cells and fibers in restricted domains within the mPFC and did not back-label cells or fibers in other parts of the cortex (Fig. 6*D* and SI Fig. 16). We observed a subset of projections oriented toward the nucleus accumbens (Fig. 6*E* and SI Fig. 16), other fibers tightly localized within the internal capsule in the medial striatum (Fig. 6*E* and SI Fig. 16), and labeling in the medial thalamus (Fig. 6*F* and SI Fig. 16). We did not observe major differences between genotypes in these labeling patterns (Fig. 6 *C′*, *D′*, *E′*, and *F′* and SI Fig. 16).

Discussion

We provide evidence that *Fgf17* has a selective function in the regionalization of FC subdivisions. Our analysis required identifying a panel of gene expression markers that distinguish dorsal and ventral subdivisions of the newborn rodent FC (Fig. 3, SI Fig. 10, Table 1, and SI Tables 2 and 3). In addition, we have characterized two lines of BAC transgenic mice that provide specific GFP labeling of the FC, and we show that they can be used as readouts of cortical regionalization and projections patterns from the FC (Figs. 2, 3, and 5 and SI Figs. 10, 13, and 14). The expression pattern of many of these genes revealed distinct borders within the FC at birth, suggesting a genetic partitioning of this cortical region before overt cytoarchitectonic differentiation. Although expression of none of the genes was limited to a single cortical region, combinations of genes were useful in defining regional subdivisions that correlated with histologically defined cortical areas (Table 1).

The lack of overt forebrain morphologic defects in *Fgf17*$^{-/-}$ mutants and the mildly reduced cortical surface area in the adult (SI Fig. 8) show that *Fgf17* does not have a major effect on forebrain growth. Rather, the results suggest that *Fgf17* has a more specific function in regulating regional specification, par-

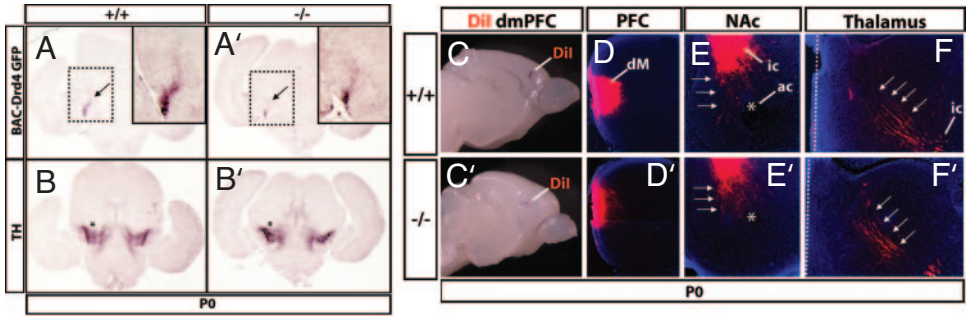

Fig. 6. FC connectivity in *Fgf17*$^{-/-}$ mice. (*A* and *A′*) Reduction in FC projections to the ventral midbrain revealed by anti-GFP immunohistochemistry on P0 coronal sections from *Fgf17*$^{+/+}$ and *Fgf17*$^{-/-}$ mice containing the BAC-Drd4 GFP transgene. Note the reduced staining of fibers emanating from the cerebral peduncle (arrows). *Insets* show magnified views of the boxed areas. (*B* and *B′*) Anti-tyrosine hydroxylase (TH) immunohistochemistry on sections adjacent to those shown in *A* and *A′*. Staining of the substantia nigra pars compacta and ventral tegmental area (asterisks) was similar between genotypes. (*C* and *C′*) DiI crystal placements in the dorsomedial FC of P3 *Fgf17*$^{+/+}$ and *Fgf17*$^{-/-}$ brains viewed from the medial side. (*D* and *D′*) Restricted DiI-labeled field in the dorsomedial (dM) PFC in coronal section rostral to the crystal placement. Medial is to the left. (*E* and *E′*) Projections to the nucleus accumbens (NAc) (arrows). Anterograde-labeled fibers in the internal capsule (ic) restricted to the ventromedial striatum are also present. The anterior commisure provides a landmark (asterisk). Medial is to the left. (*F* and *F′*) Corticothalamic fibers (arrows) emanate from the internal capsule (ic) and are present in similar locations in both genotypes. A dotted line designates the thalamic midline.

ticularly within the FC. By contrast, severe reductions in *Fgf8* levels result in gross forebrain morphologic defects that are likely due to a combination of abnormal regional specification, decreased proliferation, and increased apoptosis (15, 16). In addition to spatiotemporal differences in *Fgf8* and *Fgf17* expression (17) (Fig. 1), differences in ligand affinity for FGF receptors and ability to regulate gene expression may explain the differences in phenotypic effects (21, 22).

The $Fgf17^{-/-}$ mutant displays a rostral shift of caudal cortical areas (Fig. 4 and SI Fig. 12) that is less severe than in $Fgf8^{neo/neo}$ mildly hypomorphic mutants (14), suggesting that *Fgf17* has a more subtle role than *Fgf8* in patterning the neocortical areal map. Our postnatal analyses do not clarify whether the rostral shift in sensory cortices is only due to hypoplasia of the FC and/or due to respecification of the rostral progenitor domain to develop as more caudal cortex.

Analysis of FC subdivisions unexpectedly identified that *Fgf17* selectively regulates the sizes and positions of dorsal, but not ventral, FC subdivisions (Fig. 3 and SI Figs. 10 and 11). In $Fgf8^{neo/neo}$ mutants both the dorsal and ventral FC are reduced (ref. 14 and J.A.C. and J.L.R.R., unpublished data). These phenotypic differences may be explained in part by the observations that (*i*) *Fgf17* was expressed in a broader domain in the rostral patterning center than *Fgf8* (particularly in its dorsal extent), and (*ii*) *Fgf8* expression was normal in the $Fgf17^{-/-}$ embryonic brain (Fig. 1). We propose that reduced FGF signaling specifically in the dorsal part of the rostral patterning center could selectively affect dorsal FC regionalization while preserving the ventral FC. Current evidence, which is consistent with the protomap model, suggests that FGFs produced by the rostral patterning center regulate the regional expression of transcription factors in the neuroepithelium to specify cortical areal identity (4–7).

The neocortex of $Fgf17^{-/-}$ mutants shows correct area-specific thalamic innervation, as exemplified by the presence of somatosensory barrels, detected by both cytochrome oxidase staining and serotonin immunohistochemistry at P7 (Fig. 4). However, the position of the somatosensory barrel fields is shifted rostrally, showing that thalamocortical innervation shifts in concert with the shift in areal molecular markers. In both the $Fgf17^{-/-}$ and $Fgf8^{neo/neo}$ mutants, there was no detectable difference in thalamocortical innervation at P0 (14) (SI Fig. 16 and data not shown). Ectopic *Fgf8* expression experiments, which result in viable animals, suggest that rerouting of thalamocortical axons to area-specific targets occurs postnatally within the cortex (23). This could account for the rostral shift of the innervation of somatosensory barrel fields in the $Fgf17^{-/-}$ mutant.

Recent evidence suggests that *Fgf8* plays a role in regulating patterns of intracortical connectivity (24). Unlike in the $Fgf8^{neo/neo}$ mutant, we found no evidence for ectopic rostral projections of caudally located cortical neurons in the $Fgf17^{-/-}$ brain (data not shown), consistent with the subtler phenotype of the $Fgf17^{-/-}$ mutants.

Although $Fgf17^{-/-}$ mutants did not show an overt qualitative defect in dorsomedial FC connectivity/projections (Fig. 6 and SI Fig. 16), there was evidence for a quantitative reduction in its subcortical projections based on BAC-EphA2 and BAC-Drd4 GFP expression in the striatum and ventral midbrain, respectively (Figs. 5 and 6 and SI Figs. 13 and 15). We propose that this is secondary to a reduction in the number of FC-specified neurons. Reduced PFC output to striatal or midbrain dopaminergic neurons may have important physiologic ramifications for the regulation of neural pathways involved in reward, cognition, and social behavior (25–29).

Dorsal and ventral FC subdivisions have distinct roles in regulating cognition and behavior in rodents (3, 26) and primates including humans (25, 30, 31). For example, subdivisions of the dorsal PFC are implicated in working memory, attention, response selection, temporal processing of information, effort-related decision making, and social valuation, whereas ventromedial and orbital subdivisions are implicated in behavioral flexibility, emotional regulation, delay-related decision making, evaluation of rewards, and autonomic control (1, 3, 25, 26, 29, 30, 32–34). Therefore, the $Fgf17^{-/-}$ mutant provides a unique opportunity to examine the behavioral and neurophysiologic consequences of an early developmental genetic lesion that selectively affects the dorsal FC. We have identified circumscribed behavioral deficits in $Fgf17^{-/-}$ mutants that affect social interactions (K. Scearce-Levie, E. Roberson, J.A.C., J.L.R.R., and L. Mucke, unpublished data). We propose that elucidating the signaling pathways downstream of *Fgf17* will provide important insights into the genetic pathways that regulate FC development and that may be disrupted in disorders that affect cognition, emotion, and social interactions.

Methods

Detailed Methods. *SI Methods* contains a more detailed description of methods used.

Animals and Tissue Preparation. All mice were housed and handled in accordance with the Institutional Animal Care and Use Committee of the University of California, San Francisco. $Fgf17^{-/-}$ mice and embryos were generated by mating male and female heterozygotes ($Fgf17^{+/-}$) (17). BAC transgenic lines BAC-Drd4 GFP and BAC-EphA2 GFP (18) were mated to $Fgf17^{-/-}$ mice to generate double heterozygotes, which were then crossed to $Fgf17^{+/-}$ mice to generate $Fgf17^{+/+}$ and $Fgf17^{-/-}$ BAC transgene-positive littermates. All tissue was harvested, fixed, and cryopreserved according to standard methods. Sections were cut on either a cryostat or a freezing microtome.

ISH and Immunohistochemistry. Digoxigenin-labeled riboprobes were generated for the following genes: *Cadherin-6*, *Cadherin-8* (35), *Fgf8* (36), *Fgf17* (10), *Id-2* (35), *Lmo3*, and *Lmo4* (37), *Neurogenin-2* (38), *Neurotrophin-3* (gift from Luis Parada, UT Southwestern, Dallas, TX), *RZR-β* (35), and *Steel* (gift from E. Grove, University of Chicago, Chicago, IL). Section and whole-mount ISH were performed as described previously in refs. 35 and 19, respectively.

Immunohistochemistry was performed by using standard protocols (35) with rabbit anti-GFP (1:1,000; Invitrogen, Carlsbad, CA), rabbit anti-tyrosine hydroxylase (1:500; Chemicon, Temecula, CA), rabbit anti-serotonin (1:50,000; Immunostar, Hudson, WI) antibodies and detected with goat anti-rabbit biotinylated secondary antibody (1:200–1:400; Vector Laboratories, Burlingame, CA) and the ABC kit (Vector Laboratories).

Axon Tracing. P0–P3 brains were stored in 4% PFA in PBS at 4°C. Single crystals of the fluorescent carbocyanide dye DiI (Invitrogen) were placed in various cortical locations (39). After diffusion, sections were cut on a vibratome and immediately mounted on slides using Vectashield mounting medium with DAPI (Vector Laboratories).

Digital Imaging and Quantification of Cortical Areas. Whole brains and sections were photographed by using SPOT (Diagnostic Instruments, Sterling Heights, MI) and Olympus digital cameras and imaging software. Areas were determined by using photos of dorsally viewed whole-mount brains in ImageJ (National Institutes of Health, Bethesda, MD). Excel (Microsoft, Redmond, WA) was used for calculations and statistical analysis.

We thank David Ornitz for providing the *Fgf17* mice; Kimberly Scearce-Levie, Erik Roberson, Lennart Mucke, and members of the J.L.R.R.

laboratory for insightful discussion and valuable comments regarding the manuscript; and Dianna Kahn for technical assistance. This work was supported by the Medical Scientist Training Program of the University of California, San Francisco (J.A.C.); Nina Ireland (J.L.R.R.); the Larry L. Hillblom Foundation (J.L.R.R.); and National Institutes of Health Grants NS34661-01A1 and K05 MH065670 (both to J.L.R.R.).

1. Fuster JM (2001) *Neuron* 30:319–333.
2. Uylings HB, Groenewegen HJ, Kolb B (2003) *Behav Brain Res* 146:3–17.
3. Heidbreder CA, Groenewegen HJ (2003) *Neurosci Biobehav Rev* 27:555–579.
4. Rakic P (1988) *Science* 241:170–176.
5. O'Leary DD, Nakagawa Y (2002) *Curr Opin Neurobiol* 12:14–25.
6. Grove EA, Fukuchi-Shimogori T (2003) *Annu Rev Neurosci* 26:355–380.
7. Sur M, Rubenstein JL (2005) *Science* 310:805–810.
8. Maruoka Y, Ohbayashi N, Hoshikawa M, Itoh N, Hogan BL, Furuta Y (1998) *Mech Dev* 74:175–177.
9. Hoshikawa M, Ohbayashi N, Yonamine A, Konishi M, Ozaki K, Fukui S, Itoh N (1998) *Biochem Biophys Res Commun* 244:187–191.
10. Xu J, Lawshe A, MacArthur CA, Ornitz DM (1999) *Mech Dev* 83:165–178.
11. Bachler M, Neubuser A (2001) *Mech Dev* 100:313–316.
12. Fukuchi-Shimogori T, Grove EA (2001) *Science* 294:1071–1074.
13. Fukuchi-Shimogori T, Grove EA (2003) *Nat Neurosci* 6:825–831.
14. Garel S, Huffman KJ, Rubenstein JL (2003) *Development (Cambridge, UK)* 130:1903–1914.
15. Storm EE, Rubenstein JL, Martin GR (2003) *Proc Natl Acad Sci USA* 100:1757–1762.
16. Storm EE, Garel S, Borello U, Hebert JM, Martinez S, McConnell SK, Martin GR, Rubenstein JL (2006) *Development (Cambridge, UK)* 133:1831–1844.
17. Xu J, Liu Z, Ornitz DM (2000) *Development (Cambridge, UK)* 127:1833–1843.
18. Gong S, Zheng C, Doughty ML, Losos K, Didkovsky N, Schambra UB, Nowak NJ, Joyner A, Leblanc G, Hatten ME, Heintz N (2003) *Nature* 425:917–925.
19. Hamasaki T, Leingartner A, Ringstedt T, O'Leary DD (2004) *Neuron* 43:359–372.
20. Noain D, Avale ME, Wedemeyer C, Calvo D, Peper M, Rubinstein M (2006) *Eur J Neurosci* 24:2429–2438.
21. Olsen SK, Li JY, Bromleigh C, Eliseenkova AV, Ibrahimi OA, Lao Z, Zhang F, Linhardt RJ, Joyner AL, Mohammadi M (2006) *Genes Dev* 20:185–198.
22. Liu A, Li JY, Bromleigh C, Lao Z, Niswander LA, Joyner AL (2003) *Development (Cambridge, UK)* 130:6175–6185.
23. Shimogori T, Grove EA (2005) *J Neurosci* 25:6550–6560.
24. Huffman KJ, Garel S, Rubenstein JL (2004) *J Neurosci* 24:8917–8923.
25. Goldman-Rakic PS (1996) *Proc Natl Acad Sci USA* 93:13473–13480.
26. Dalley JW, Cardinal RN, Robbins TW (2004) *Neurosci Biobehav Rev* 28:771–784.
27. Young LJ, Wang Z (2004) *Nat Neurosci* 7:1048–1054.
28. Meyer-Lindenberg A, Kohn PD, Kolachana B, Kippenhan S, McInerney-Leo A, Nussbaum R, Weinberger DR, Berman KF (2005) *Nat Neurosci* 8:594–596.
29. Kellendonk C, Simpson EH, Polan HJ, Malleret G, Vronskaya S, Winiger V, Moore H, Kandel ER (2006) *Neuron* 49:603–615.
30. Price JL (2006) *Prefrontal Cortex* (CRC Press, Boca Raton, FL).
31. Amodio DM, Frith CD (2006) *Nat Rev Neurosci* 7:268–277.
32. Rudebeck PH, Buckley MJ, Walton ME, Rushworth MF (2006) *Science* 313:1310–1312.
33. Rudebeck PH, Walton ME, Smyth AN, Bannerman DM, Rushworth MF (2006) *Nat Neurosci* 9:1161–1168.
34. Mitchell JP, Macrae CN, Banaji MR (2006) *Neuron* 50:655–663.
35. Rubenstein JL, Anderson S, Shi L, Miyashita-Lin E, Bulfone A, Hevner R (1999) *Cereb Cortex* 9:524–532.
36. Crossley PH, Martin GR (1995) *Development (Cambridge, UK)* 121:439–451.
37. Bulchand S, Subramanian L, Tole S (2003) *Dev Dyn* 226:460–469.
38. Fode C, Gradwohl G, Morin X, Dierich A, LeMeur M, Goridis C, Guillemot F (1998) *Neuron* 20:483–494.
39. Godement P, Vanselow J, Thanos S, Bonhoeffer F (1987) *Development (Cambridge, UK)* 101:697–713.
40. Zilles K, Wree A (1995) in *The Rat Nervous System*, ed Paxinos G (Academic Press, San Diego), pp 649–685.
41. Krettek JE, Price JL (1977) *J Comp Neurol* 171:157–191.